DOI 10.1007/s12182-014-0318-5

# Control of hydrocarbon accumulation by Lower Paleozoic cap rocks in the Tazhong Low Rise, Central Uplift, Tarim Basin, West China

**Zhang Yanping[1, 2], Lü Xiuxiang[1, 2*], Yang Haijun[3], Han Jianfa[3], Lan Xiaodong[1, 2], Zhao Yue[3] and Zhang Jinhui[4]**

[1] College of Geosciences, China University of Petroleum, Beijing 102249, China
[2] State Key Laboratory of Petroleum Resources and Prospecting, China University of Petroleum, Beijing 102249, China
[3] Tarim Oilfield Company, PetroChina, Korla, Xinjiang 841000, China
[4] CNOOC Tianjin Branch Company, Tianjin 300452, China



**Abstract:** Despite the absence of regional cap rocks in the Lower Paleozoic for the entire Tazhong Low Rise, several sets of effective local cap rocks are well preserved on the Northern Slope. Of these the best is the Ordovician mudstone of the Sangtamu Formation; the second is the Silurian Red Mudstone Member of the Tatairtag Formation and the marl of the Ordovician Lianglitag Formation; and the third is the gray mudstone of the Silurian Kepingtag Formation. The dense limestone of the Ordovician Yingshan Formation and the gypsum of the Middle Cambrian have shown initial sealing capacity. These effective cap rocks are closely related to the distribution of Lower Palaeozoic hydrocarbons in the Tazhong Low Rise. With well-preserved Sangtamu Formation mudstone and its location close to migration pathways, rich Lower Paleozoic hydrocarbon accumulation can be found on the Northern Slope. Vertically, most of the reserves are distributed below the Sangtamu Formation mudstone; areally, hydrocarbons are mainly found in the areas with well-developed Sangtamu Formation mudstone and Lianglitag Formation marl. Burial history and hydrocarbon charging history show that the evolution of Lower Palaeozoic cap rocks controlled the accumulation of hydrocarbon in the Tazhong Low Rise. Take the Red Mudstone Member of the Tatairtag Formation and Sangtamu Formation mudstone for examples: 1) In the hydrocarbon charging time of the Late Caledonian − Early Hercynian, with top surfaces at burial depths of over 1,100 m, the cap rocks were able to seal oil and gas; 2) During the intense uplifting of the Devonian, the cap rocks with top surfaces at burial depths of 200-800 m and 500-1,100 m respectively were denuded in local areas, thus hydrocarbons trapped in earlier time were degraded to widespread bitumen; 3) In the hydrocarbon charging time of the Late Hercynian and Himalayan, the top surfaces of the cap rocks were at burial depths of over 2,000 m without intense uplifting and denudation thereafter, so trapped hydrocarbons were preserved. Based on cap rocks, the Ordovician Penglaiba Formation and Lower Cambrian dolomite could be potential targets for exploration on the Tazhong Northern Slope, and combined with hydrocarbon migration, less risk would be involved.

**Key words:** Cap rock, hydrocarbon accumulation, hydrocarbon destruction, Lower Paleozoic, Tazhong Low Rise

## 1 Introduction

Cap rocks play an important role in oil and gas preservation in hydrocarbon-bearing areas with strong tectonic activities. For instance, although the Papuan Fold & Thrust Belt of the Papua Basin experienced strong compression and deformation with plenty of seeps, over two billion barrels of recoverable oil equivalent were discovered; the biggest Hides field had over 1,800 m gas column height, and the key is the sealing and plastic adjustment from Cretaceous mudstone cap rocks with around 1,000 m thickness (Hill, 1991; Hill et al, 2004). The Maracaibo Basin was located on the edge of plate convergence and experienced complex tectonic activities, with many oil seeps surrounding the basin. Still 44 billion barrels of recoverable oils were preserved, mainly owing to multiple sets of mudstone cap rocks (Escalona and Mann, 2006). The Kela 2 gas field, the most productive in China, is located in the highly deformed thrust belt of the Tarim Basin, and its formation is mainly due to high-quality Eogene evaporite regional cap rocks (Jia and

*Corresponding author. email: luxx@cup.edu.cn
Received December 6, 2012

Li, 2008).

The Tarim Basin, a typical superimposed basin with long-term evolution in west China, experienced multi-phase tectonic movements, multi-phase hydrocarbon expulsion (Gong et al, 2007; Zhang et al, 2011c; Tian et al, 2012), multi-phase oil & gas accumulation (Li et al, 1996; Jin and Wang, 2004; Meng et al, 2008; Pang et al, 2010), and multiple adjustment and destruction of hydrocarbon reservoirs (Lü et al, 1997). The Tazhong Low Rise is one of the petroliferous areas in the Tarim Basin, and experienced complex processes of hydrocarbon accumulation, adjustment and destruction (Jiang et al, 2008; Pang et al, 2013), thus research on cap rocks and preservation of hydrocarbons is important. However, the previous research on petroleum geology in the Tazhong Low Rise focused on source rocks and reservoir beds (Zhang et al, 2000; Li et al, 2009; Ding et al, 2012), and the Lower Palaeozoic cap rocks were less studied. In addition, the oil and gas discovered in the Tazhong Low Rise were mostly located in the Lower Palaeozoic, thus the relationship of hydrocarbon accumulation with the Lower Palaeozoic cap rocks can be instructive to exploration in the Tazhong Low Rise.

# 2 Geologic setting

## 2.1 Geologic structures in the Tazhong Low Rise

The Tazhong Low Rise with an area of 27,500 km$^2$ is located in the heartland of the Central Uplift of the Tarim Basin, and is adjacent to the Manjiaer Sag in the northeast with the Tazhong No.1 Fault as its border, the Awati Sag in the northwest, the Bachu Salient in the west with the Tumuxiuke Fault as borders, the Tangguzibasi Sag in the south and the Tadong Low Rise in the east (Fig. 1). Structural research shows that the Tazhong Low Rise with the eastern structure higher than the western one at present is a large complete NWW trending anticline structure with several secondary structural zones. From north to south, several fault belts were developed, namely the Tazhong No.1 Fault Belt, Tazhong No.10 Fault Belt, Tazhong No.2 Fault Belt, and the Tazhong Southern Fault Belt. In the plane, the fault systems spread to the west and converge to the east near the TZ5 well block (Fig. 1).

The Tazhong Low Rise is a pre-Carboniferous uplifted

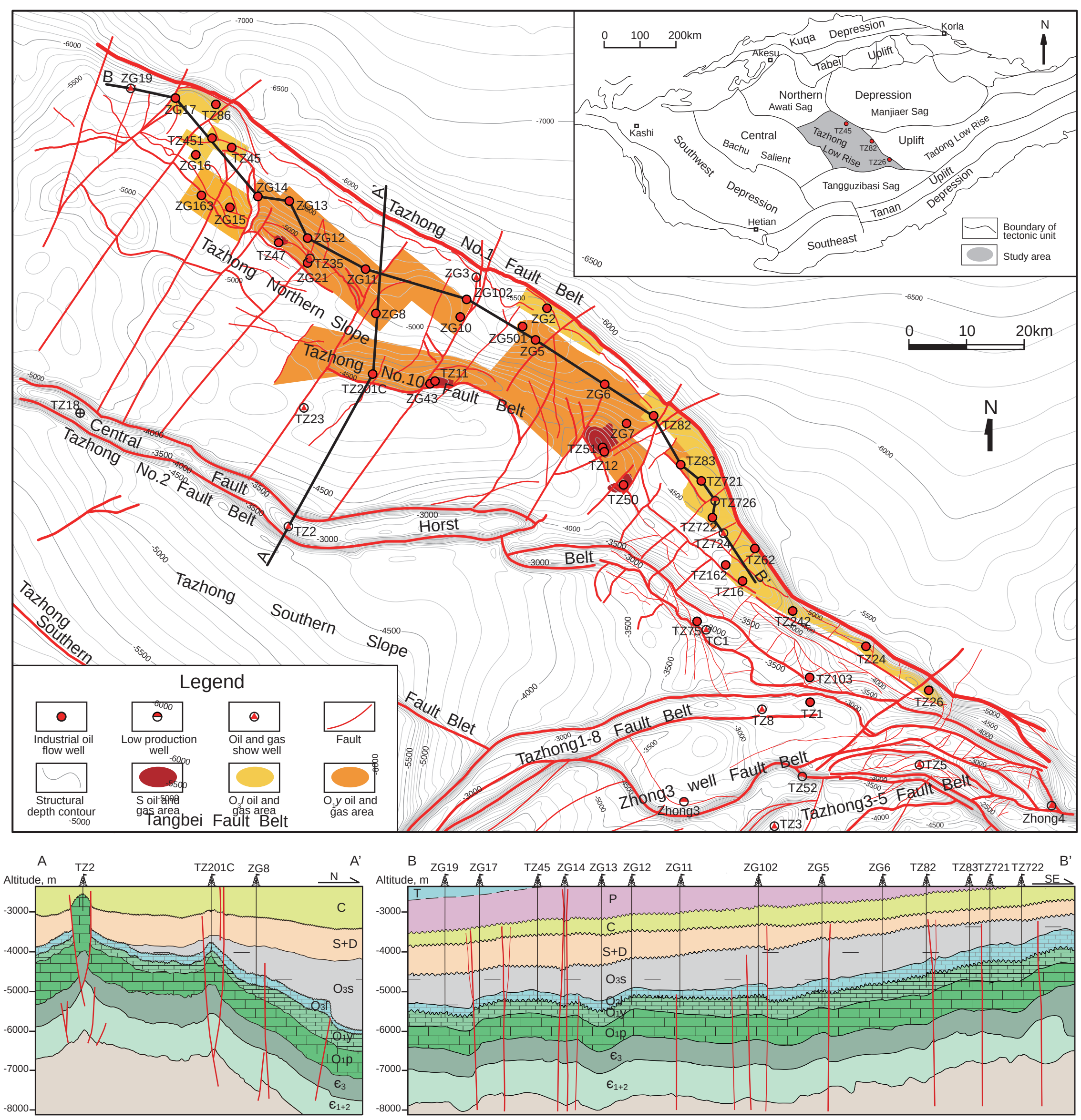

Fig. 1 Geologic configuration of the Tazhong Low Rise

structure in the Paleozoic craton basin of the Tarim Basin. Tectonic activities on the southern basin margin played an important role in controlling the formation and development of Tazhong structures. According to stratigraphic development, structural deformation, unconformities and regional geology, the structural evolution in the Tazhong Low Rise can be divided into four stages (Jia, 1997): 1) Formation of rudimental structure (Sinian-Ordovician); 2) Thrust, strike-slip structural deformation and structural finalization (Silurian-Devonian); 3) Development of giant nose-shaped uplift (Carboniferous-Permian); 4) Stable subsidence and uplifting (Triassic-Quaternary).

### 2.2 Reservoir bed–seal combination in the Lower Paleozoic

The Silurian, Ordovician and Cambrian are developed in the Lower Paleozoic in the Tazhong Low Rise (Fig. 2).

In the Silurian, sandstones and mudstones were deposited in the Tatairtag Formation ($S_2t$) and Kepingtag Formation ($S_1k$). The lower member of $S_2t$ is called Red Mudstone Member ($S_2t$-*rmm*) and is a premium cap rock for the Silurian oil and gas. The upper member of $S_1k$ is further divided into 1st, 2nd and 3rd sub-members from top to bottom, the upper 2nd sub-member consists of gray mudstones and is called Gray Mudstone Sub-member ($S_1k$-*gms*) while the upper 1st and 3rd sub-members are both mainly composed of sandstone, thus the $S_2t$-*rmm* can seal the upper 1st sub-member of $S_1k$ while the $S_1k$-*gms* can seal the upper 3rd sub-member of $S_1k$.

In the Ordovician, the Sangtamu Formation ($O_3s$) mainly consists of mudstone, while the underlying Lianglitag ($O_3l$), Yingshan ($O_1y$) and Penglaiba Formations ($O_1p$) mainly consist of carbonate rocks. $O_3s$ is a premium cap rock for Ordovician hydrocarbons and direct cap rock for the hydrocarbons in $O_3l$ limestones of reef-flat facies; the muddy limestone in the 3rd to 5th members of $O_3l$ could be cap rock for the underlying weathering crust karst reservoir beds along the top part of $O_1y$; the thick dense limestone without weathering and karstification in the $O_1y$ is cap rock for underlying $O_1p$ hydrocarbons.

In the Cambrian (∈) with upper dolomite member, gypsum member and lower dolomite member, the gypsum member can seal hydrocarbon in the lower dolomite member.

In the structural highs of the Tazhong Low Rise, the Carboniferous directly overlay the Ordovician (such as in the TZ2 well), and even the Cambrian (such as in the TZ1 well) as the result of strong denudation.

## 3 Features of Lower Paleozoic cap rocks

### 3.1 Red Mudstone Member in the Silurian ($S_2t$-*rmm*)

The $S_2t$-*rmm* mudstone is a set of cap rocks widely distributed in the Tazhong Low Rise, Manjiaer Sag and the southwest area of the Tabei Uplift.

The $S_2t$-*rmm* in the Tazhong Low Rise mainly consists of tidal flat facies brown mudstone, with an average total thickness of 70 m (29-109 m) and single layer thickness of 15-80 m. Areally, the $S_2t$-*rmm* mudstone gradually becomes thicker from southeast to northwest, but was completely denuded at the east end of the Tazhong Low Rise and the Central Fault Horst Belt because of uplifting (Fig. 3). It is in sub-stage A of the middle diagenetic stage, because authigenetic clay minerals in the TZ23 well at 4,774 m near the bottom of $S_2t$-*rmm* are dominated by 75% illite-smectite (I/S), 15% illite and 10% kaolinite, and 20% smectite in I/S (S%) (Zhang et al, 2011c), and the Silurian vitrinite reflectance ($R_o$) is 0.9%-1.3%. Its breakthrough pressure ranges from 15.1 MPa to 25.1 MPa in four testing samples saturated with water (Wang et al, 2004).

### 3.2 Gray Mudstone Sub-member in the Silurian ($S_1k$-*gms*)

$S_1k$-*gms* in the Tazhong Low Rise is mainly composed of tidal flat facies gray mudstone, with an average total thickness of 18 m (8-35 m) and single layer thickness of 1-10 m, and thinner than the $S_2t$-*rmm*. Areally, $S_1k$-*gms* mudstone also gradually becomes thicker from south to north, but completely eroded at the east end of the Tazhong Low Rise and the Central Fault Horst Belt due to uplifting (Fig. 4).

It is also in sub-stage A of the middle diagenetic stage, because authigenetic clay minerals of the TZ37 well at 4,679.93 m near the bottom of $S_1k$-*gms* are dominated by 78% illite–smectite, 15% illite, 4% kaolinite and 3% chlorite, and 25% smectite in I/S (S%) (Zhang et al, 2011c). The breakthrough pressures are more than 15.1 MPa in all four testing samples saturated with water (Wang et al, 2004), thus it is able to seal the 3rd sub-member of $S_1k$ (Lü et al, 2007).

### 3.3 Mudstone of Ordovician Sangtamu Formation ($O_3s$)

Previous research shows that the Lower Mudstone Member of the Carboniferous is a good regional cap rock in the Tarim Basin, which covers a giant hydrocarbon accumulation system. However, exploration progress shows that around 80% of oil and gas reserves accumulate below $O_3s$ mudstone, thus it actually plays the most important role in sealing oil and gas in the Tazhong Low Rise.

During the deposition of $O_3s$ with subsidence of the entire Tazhong area, the thick mudstone of shelf slope and deep water basin facies was deposited with an average total thickness of 570 m (100-1,100 m) and single layer thickness of 50-130 m. Areally, $O_3s$ mudstone gradually becomes thicker from the Central Fault Horst Belt to both sides with broad lateral distribution, but completely denuded in the Central Fault Horst Belt and the east end of the Tazhong Low Rise due to uplifting (Fig. 5). The displacement pressures of $O_3s$ mudstone range from 6.7 MPa to 37.1 MPa with an average of 15.3 MPa (Zhu et al, 2003).

According to statistics from 114 wells in the Tazhong Low Rise, the bottom depth of $O_3s$ ranges from 3,825 m to 6,830 m with an average of 5,200 m; the 3,682-4,500 m of $O_3s$ in the TZ28 well has $R_o$ values of 1.03%-1.32%; the 5,415-5,420 m of $O_3s$ in the TZ35 well has the $T_{max}$ of 445-455 °C, while the 4,917-5,101 m of TZ10 well has the $T_{max}$ of 428-443 °C. The clay minerals of Zhong13 well at 5,219 m in the $O_3s$ are dominated by 78% illite, 5% kaolinite, 15% chlorite and 2% illite–smectite (I/S), and 15% (S%) in I/S (Qian et al, 2012).

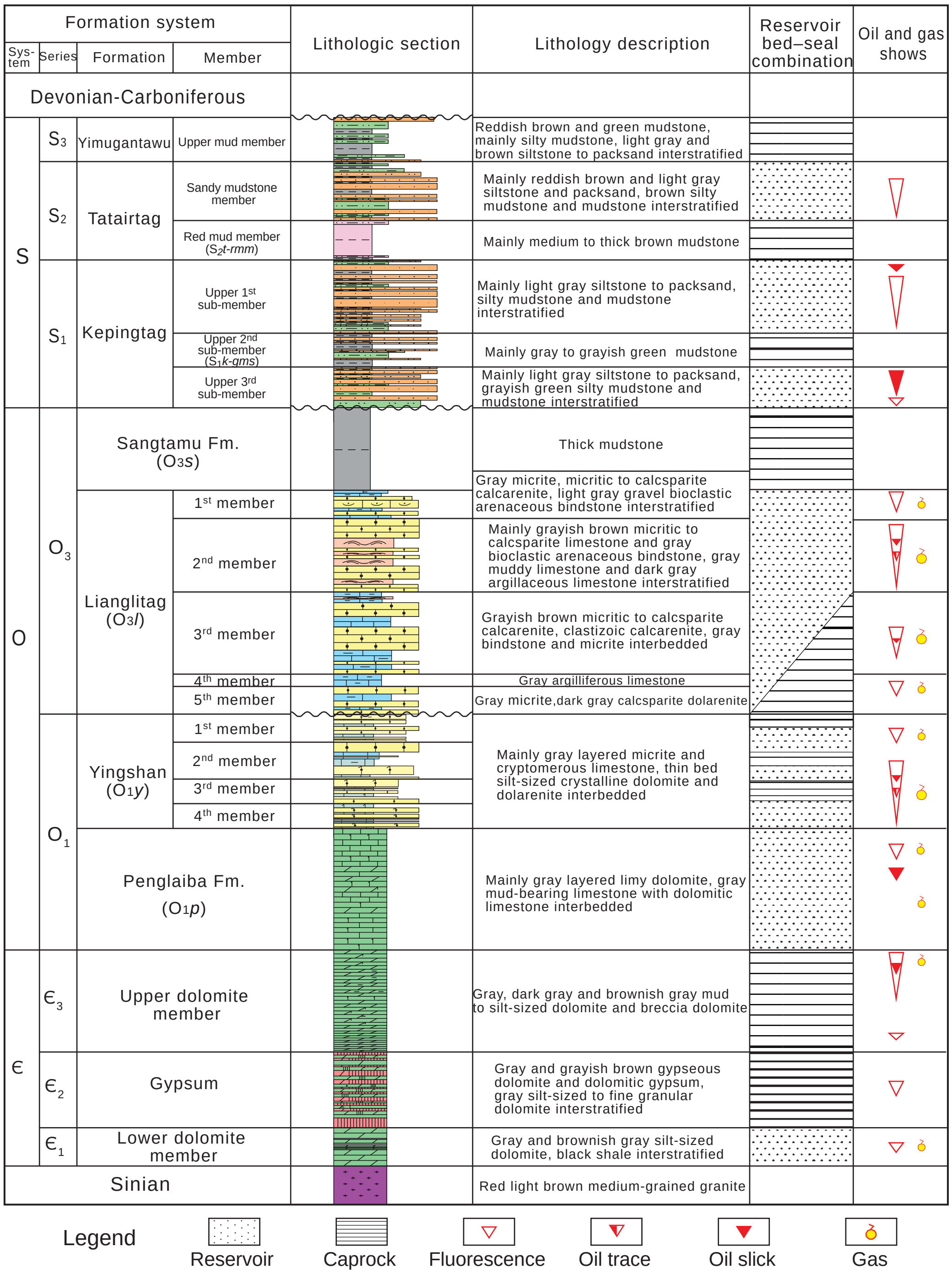


Fig. 2 Stratigraphic column showing Lower Paleozoic reservoir bed–seal combination in the Tazhong Low Rise

$O_3s$ in most areas of the Tazhong Low Rise is in sub-stage $A_2$ of the late diagenetic stage.

### 3.4 Marl of Ordovician Lianglitag Formation ($O_3l$)

$O_3s$ mudstone is the direct cap rock for oil and gas in the underlying $O_3l$. In addition, hydrocarbon accumulation in reservoir beds of weathering crust karst was discovered in $O_1y$ below $O_3l$. However, $O_1y$ in most parts of the Tazhong Low Rise is far below $O_3s$ mudstone at more than a few hundred meters, thus dense marl in the 3rd to 5th members of $O_3l$ directly seals the hydrocarbons in $O_1y$.

The dense marl in the 3rd to 5th members of $O_3l$ is a set of reef-flat complex sediments on a carbonate platform–shelf margin with an average total thickness of 220 m (100-400 m) and single layer thickness of 5-80 m. Areally, it gradually becomes thicker from the Central Fault Horst Belt to both sides with wide lateral distribution, but thinner in the ZG15-ZG24 well blocks with the 4th and 5th members of $O_3l$ missing. In addition, it was also completely eroded in the Central Fault Horst Belt and the east end of the Tazhong Low Rise due to uplifting (Fig. 6). According to testing of dense marl cap rocks in 13 wells, no breakthrough occurred in 85%

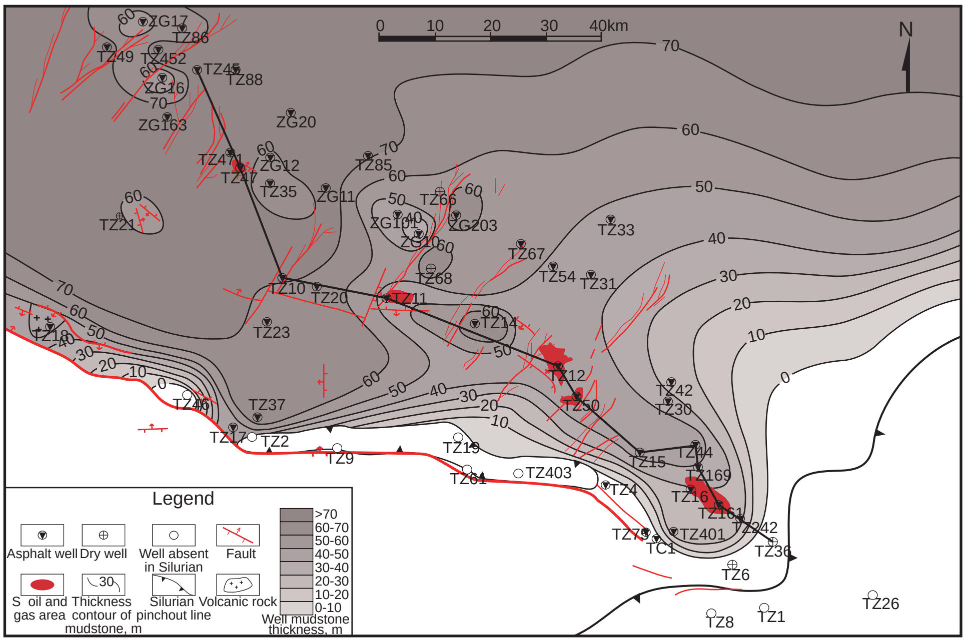


Fig. 3 Mudstones isopach map of $S_2$*t-rmm*

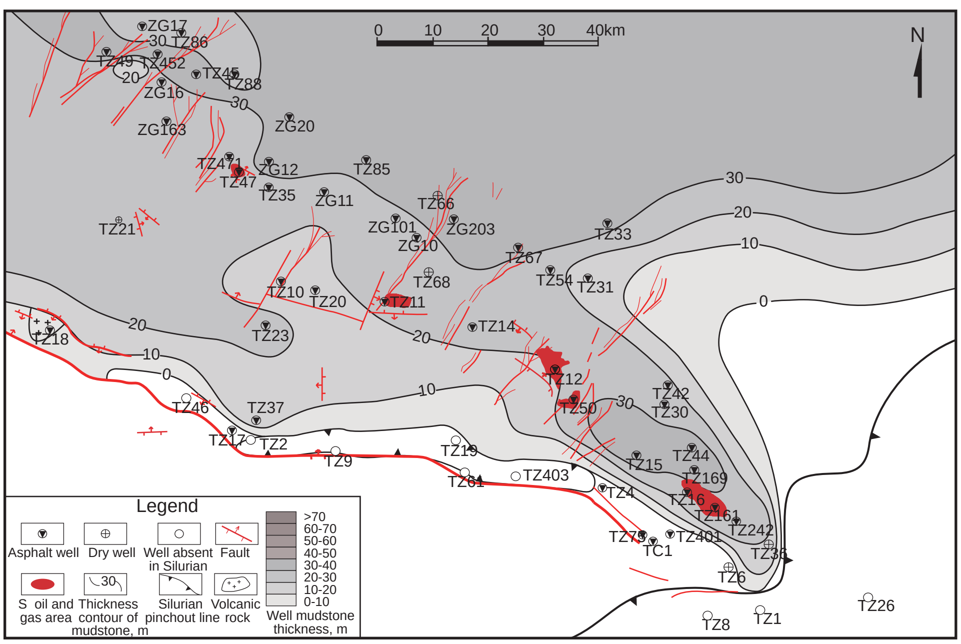


Fig. 4 Mudstones isopach map of $S_1$*k-gms*

of samples after 48 hours under 14 MPa applied maximum pressure, while the two remaining samples respectively had the breakthrough pressure of 7 MPa and 10 MPa (Table 1).

According to statistics from 38 wells in the Tazhong Low Rise, the bottom depth of $O_3l$ ranges from 4,033 m to 7,102 m with an average of 5,474 m. The homogenization temperatures of hydrocarbon inclusions range from 67 °C to 125 °C in the 3,976-6,099 m of $O_3l$ from the TZ6, TZ12, TZ45 wells (Chen et al, 2010). According to PVT reports of 28 wells in the Tazhong Low Rise, the current formation temperatures of the 4,387-6,500 m in $O_3l$ range from 126 °C to 151 °C with an average of 139 °C. The vitrinite reflectance equivalent (VRE) values of $O_3l$ range from 0.8% to 1.3% in the Zhong12, Zhong13, TZ10, TZ12 wells (Wang et al, 2001). $O_3l$ in most areas of the Tazhong Low Rise is in sub-stage $A_2$ of the middle diagenetic stage, while in a few areas with deeper burial it entered sub-stage B of the middle diagenetic stage.

Thus the dense marl from the 3rd to 5th members of $O_3l$ can seal the underlying hydrocarbons of $O_1y$.

### 3.5 Dense limestone of Ordovician Yingshan Formation ($O_1y$)

A large amount of drilling and seismic reservoir prediction

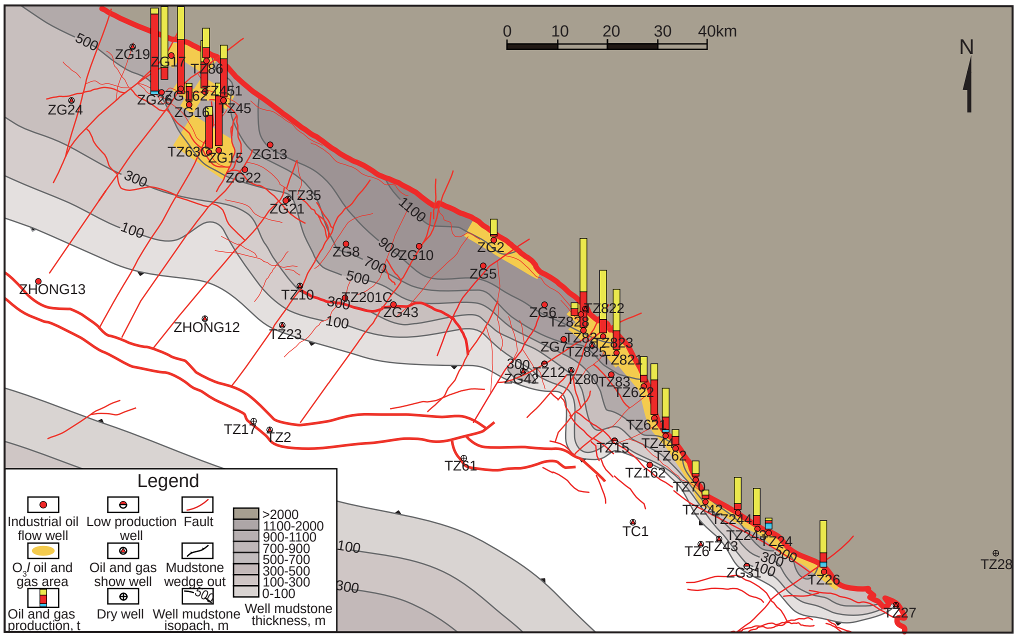


Fig. 5 $O_3s$ mudstone isopach map with oil and gas in $O_3l$

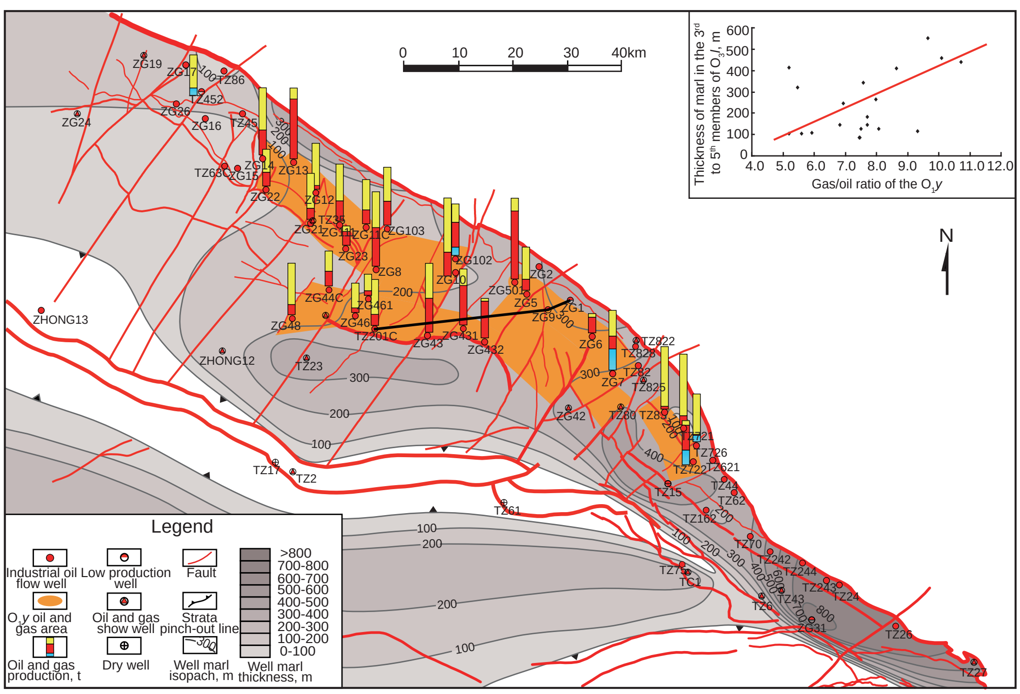


Fig. 6 Dense marl isopach map of the 3rd to 5th members of $O_3l$ with oil and gas in $O_1y$

data in the Tazhong Low Rise show that good carbonate reservoir beds of weathering crust karst in $O_1y$ mainly developed below the top surface of $O_1y$ within 120 m, with a depth of 180 m in local areas (Ji et al, 2012). Thus the thick dense limestone below the karst reservoir bed can seal the underlying hydrocarbons of $O_1p$.

Due to uplifting and denudation before the deposition of $O_3l$, most areas of the Tazhong Low Rise lost the 1st and 2nd members of $O_1y$ and the 3rd and 4th members of $O_1y$ remained, and only platform margin and slope areas had relatively well-preserved $O_1y$. $O_1y$ is partially preserved and becomes thicker from Tazhong No.2 Fault to Tazhong No.1 Fault (Fig. 7). For instance, in the TZ162 well near the Tazhong No.1 Fault $O_1y$ has a thickness of 703 m, while in the TZ75 well near the Tazhong No.2 Fault $O_1y$ thins to 202 m. Thus the northeast part of the Tazhong Northern Slope has thicker limestone in $O_1y$ without weathering and karstification, where the hydrocarbons of $O_1p$ could be better sealed.

$O_1y$ consists of limestone, micrite and dolomite of open platform facies, but the relevant characteristics of the dense limestone cap rock cannot be evaluated currently, because there are few wells penetrating through $O_1y$.

Table 1 Breakthrough pressure of dense marl cap rock in the 3rd to 5th members of $O_3l$

| Well | Depth, m | $O_3l$ | Breakthrough pressure, MPa (Pressuring range: 0-14 MPa) |
|---|---|---|---|
| TZ12 | 4973.1 | 4th member | No breakthrough after 48 hours under the max pressure |
| TZ162 | 4598.6 | 4th member | No breakthrough after 48 hours under the max pressure |
| TZ27 | 4573.2 | 5th member | No breakthrough after 48 hours under the max pressure |
| TZ35 | 5775.4 | 3rd member | No breakthrough after 48 hours under the max pressure |
| TZ43 | 4647.4 | 5th member | No breakthrough after 48 hours under the max pressure |
| TZ80 | 5423.2 | 5th member | No breakthrough after 48 hours under the max pressure |
| TZ822 | 5808.4 | 3rd member | No breakthrough after 48 hours under the max pressure |
| TZ825 | 5499.1 | 5th member | No breakthrough after 48 hours under the max pressure |
| TZ83 | 5468.1 | 4th member | No breakthrough after 48 hours under the max pressure |
| ZG8 | 6745.1 | 3rd member | No breakthrough after 48 hours under the max pressure |
| ZG31 | 4133.0 | 3rd member | No breakthrough after 48 hours under the max pressure |
| ZG19 | 6601.7 | 3rd member | 7 |
| TZ63 | 6153.9 | 3rd member | 10 |

Notes: Above testing was completed by the laboratory of Langfang Branch, Research Institute of Petroleum Exploration and Development, CNPC

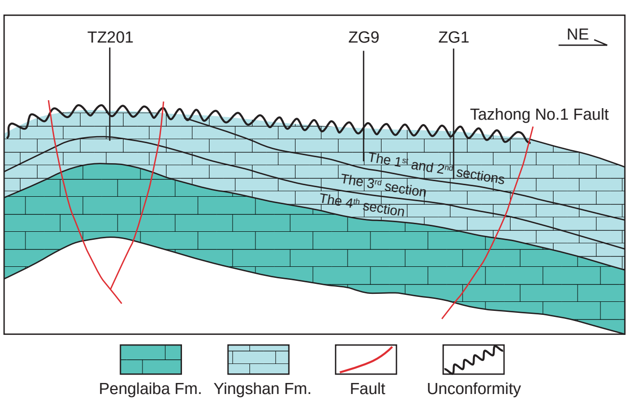


Fig. 7 Distribution of the Middle-Lower Ordovician on the Tazhong Northern Slope (see Fig. 6 for location)

### 3.6 Gypsum member of the Cambrian

The Middle Cambrian gypsum member acts as a good regional cap rock in the central-west area of the Tarim Basin, and was penetrated in the Tazhong Low Rise and Bachu Salient. In the Bachu Salient, gypsum-salt rocks of evaporite lagoon facies with a thickness of over 350 m developed at 3,822-4,379 m of the Fang-1 well and at 5,104-5,792 m of the He-4 well. In the Tazhong Low Rise, only the TC1 well penetrated through the Cambrian in the east of the Tazhong Low Rise, and the Middle Cambrian at 6,958-7,058 m is mainly composed of gypseous dolomite, dolomitic gypsum, dolomite and thin bedded gypsum, with no salt rock.

Seismic data (Tang et al, 2012) and the TC1 well data indicate that the Middle Cambrian gypsum member is preserved in the Central Fault Horst Belt and the east end of the Tazhong Low Rise where the Lower Palaeozoic was denuded, thus the gypsum member might be present in the entire Tazhong Low Rise and becomes better cap rock from east to west according to sedimentary characteristics (Zhang et al, 2012).

### 3.7 Evaluation of cap rocks in the Tazhong Low Rise

The macroscopic and microscopic evaluation criteria of cap rocks in the Tazhong Low Rise are summed up according to previous research (Table 2). Based on characteristics of Lower Palaeozoic cap rocks in the Tazhong Low Rise, the best cap rock is the $O_3s$ mudstone; secondly, the mudstone of $S_2t$-*rmm* and the marl in the 3rd to 5th members of $O_3l$; lastly, the $S_1k$-*gms* mudstone. The dense limestone of $O_1y$ and the gypsum member of Middle Cambrian ($\epsilon_2$) preliminarily show sealing capacity and their regional distribution is waiting for further study (Table 3).

## 4 Relationship of hydrocarbon accumulation and Lower Paleozoic cap rocks

In the Tazhong Low Rise, commercial oil and gas flows have been discovered in the sandstone reservoir beds of $S_1k$,

Table 2 Macroscopic evaluation criteria of cap rocks in the Tazhong Low Rise (modified from Zhu et al, 2003)

| Evaluation parameters | | Classification of cap rocks | | | |
|---|---|---|---|---|---|
| | | Class 1 | Class 2 | Class 3 | Class 4 |
| Macroscopic parameter | Sedimentary environment | Semi-deep−deep lake facies, basinal facies, open sea shelf facies | Platform facies lagoonal facies, inshore shallow lake facies, delta front sub-facies | Platform margin facies, littoral facies, delta distributary plain sub-facies | Fluvial facies, alluvial fan facies |
| | Lithology | Gypsum-salt rock mudstone, calcareous mudstone | Mudstone containing sand, mudstone containing silt | Silty mudstone, sandy mudstone, marl | Argillaceous siltstone, argillaceous sandstone |
| | Diagenetic stage | Sub-stage A of the middle diagenetic stage | Sub-stage B of the early diagenetic stage | Sub-stage B of the middle diagenetic stage sub-stage A of the early diagenetic stage | Late diagenetic stage |
| | Single layer thickness, m | >20 | 10-20 | 2.5-10 | <2.5 |
| | Cumulative thickness, m | >300 | 150-300 | 50-150 | <50 |
| Microscopic parameter | Breakthrough pressure, MPa | >15 | 15-10 | 10-5 | <5 |

Table 3 Evaluation of Lower Palaeozoic cap rocks

| Location of cap rocks | Macroscopic feature of cap rocks | Microscopic feature of cap rocks | Evaluation |
|---|---|---|---|
| Mudstone in $S_2t$-*rmm* | Mudstone of tidal flat facies, with cumulative thickness of 29-109 m and an average of 70 m, single layer thickness of 15-80 m, in sub-stage A of the middle diagenetic stage | With breakthrough pressure of 15.1-25.1 MPa | Macro: Class 2-3<br>Micro: Class 1 |
| Mudstone in $S_1k$-*gms* | Mudstone of tidal flat facies, with cumulative thickness of 8-35 m and an average of 18 m, single layer thickness of 1-10 m, in sub-stage A of the middle diagenetic stage | With breakthrough pressure of more than 15.1 MPa | Macro: Class 3<br>Micro: Class 1 |
| Mudstone in $O_3s$ | Mudstone of shelf slope facies and deep water basin facies, with a thickness of 100-1,100 m and an average of 570 m, single layer thickness of 50-130 m, in sub-stage $A_2$ of the middle diagenetic stage | With displacement pressure of 6.7-37.1 MPa and an average of 15.3 MPa | Macro: Class 1<br>Micro: Class 1 |
| Marl in $O_3l$ | Reef-flat complex limestone of platform margin and shelf margin facies, with cumulative thickness of 100-400 m and an average of 220 m, single layer thickness of 5-80 m, in the sub-stage $A_2$ of the middle diagenetic stage | No breakthrough in 85% of samples after 48 hours under 14 MPa max applied pressure | Macro: Class 2-3<br>Micro: Class 2 |
| Dense limestone in $O_1y$ | Limestone and marl of open platform facies, with cumulative thickness of 400 m in TZ162 well | No data | No evaluation |
| Gypsum in $\epsilon_2$ | Gypsum member in TC1 well at the east end of the Tazhong Low Rise developed in evaporite lagoon facies with thickness of 100 m | No data | No evaluation |

the reef-flat complex reservoir beds of $O_3l$, the weathering crust karst reservoir beds of $O_1y$ and the carbonate karst reservoir beds of $O_1p$. Around 80% of reserves in the Tazhong Low Rise are found in $O_3l$ and $O_1y$ below $O_3s$ mudstone cap rocks.

Previous research shows that there were at least three periods of large-scale hydrocarbon accumulation, including Late Caledonian−Early Hercynian, Late Hercynian, and Himalayan (Zhang et al, 2011a; Pang et al, 2013).

## 4.1 Hydrocarbon accumulation versus Silurian mudstone cap rock

Dry bitumen, asphalt, heavy oil and light oil coexist in the upper 1st and 3rd sub-members of $S_1k$ below $S_2t$-*rmm*, indicating that the sub-members experienced multiple phases of hydrocarbon charging and complex processes of accumulation and loss.

Bitumen is widely distributed in the upper 1st and 3rd sub-members of $S_1k$ in the Tazhong Low Rise (Fig. 3). It was formed from hydrocarbons charged in the Late Caledonian – Early Hercynian but degraded by Devonian uplifting (Zhang et al, 2004; 2011c). Almost all the Silurian bituminous sandstones are distributed below the $S_2t$-*rmm* cap rock, but there is no bitumen in the Silurian sandstone above the Red Mudstone Member cap rock except four wells including TZ10 well due to connection of faults (Zhang et al, 2004). This indicates that $S_2t$-*rmm* cap rock possessed sealing capacity during the early period of hydrocarbon charging and controlled the vertical distribution of hydrocarbons.

In the Silurian in the Tazhong Low Rise, there are five oil and gas reservoirs (Fig. 3), all in the upper 1st and 3rd sub-members of $S_1k$ below $S_2t$-*rmm* cap rock, while there is no hydrocarbon accumulation in Silurian sandstones above $S_2t$-*rmm* cap rock (Fig. 8). This indicates that cap rock from $S_2t$-*rm*m still controlled vertical distribution of Silurian hydrocarbons charged in late periods. In addition, Silurian movable oil is mainly found in the upper 3rd sub-member of $S_1k$ below the direct cap rock from $S_1k$-*gms*, because the upper 3rd sub-member of $S_1k$ is the oil-bearing formation of the five reservoirs. By comparison, the upper 1st sub-member of $S_1k$ is the oil-bearing formation of only two reservoirs. The reservoir bed quality of the upper 3rd sub-member of $S_1k$ is better than the upper 1st sub-member of $S_1k$. Meanwhile, the direct cap rock of the upper 3rd sub-member of $S_1k$, that is $S_1k$-*gms* possessed sealing capacity during the late period of hydrocarbon charging.

## 4.2 Hydrocarbon accumulation versus $O_3s$ mudstone cap rock

Ordovician oil and gas exploration is mainly on the Tazhong Northern Slope. There is a large oil and gas accumulation in $O_3l$ with a superimposed petroliferous area of over 1,000 km$^2$ including natural gas, condensate and normal crude oil, whose principal payzones are limestone reservoir beds of the 1st to 3rd members of $O_3l$ reef-flat complex of platform margin facies, while its direct cap rock is the $O_3s$ mudstone. Meanwhile, the $O_3s$ mudstone also plays the role of local cap rock in the Tazhong Low Rise, thus about 80% of Tazhong Low Rise's reserves are concentrated below $O_3s$.

The locations of $O_3l$ hydrocarbon reservoirs correspond well with areas of thick $O_3s$ mudstone. That is to say, firstly, hydrocarbons accumulate in the area where the mudstone cap rocks have a thickness of more than 300 m (Fig. 5); secondly, the thinner the mudstone cap rocks from northeast to southwest, the more the low productivity wells (such as the TZ15 well) and hydrocarbon show wells (such as the TZ23 and the TZ42 well) were drilled. In addition, on the top and both sides of the Central Fault Horst Belt with missing mudstone cap rocks, a number of dry wells and a few wells with only hydrocarbon shows were drilled. Therefore, the abundance of $O_3l$ hydrocarbons correlates with the thickness of overlying mudstone, although source rock, structural configuration, migration and reservoir bed quality are also factors influencing hydrocarbon distribution. It is a consensus that the sealing of thick $O_3s$ mudstone controlled regional distribution of underlying oil and gas.

## 4.3 Hydrocarbon accumulation versus $O_3l$ marl cap rock

In the Tazhong Low Rise, the weathering crust karst carbonate oil and gas reservoirs in $O_1y$ have a superimposed petroliferous area of 3,000 km$^2$ (Fig. 6). The marl of the 1st to 3rd members of $O_3l$ acts as cap rock for underlying $O_1y$, and also controls hydrocarbon accumulation in $O_1y$.

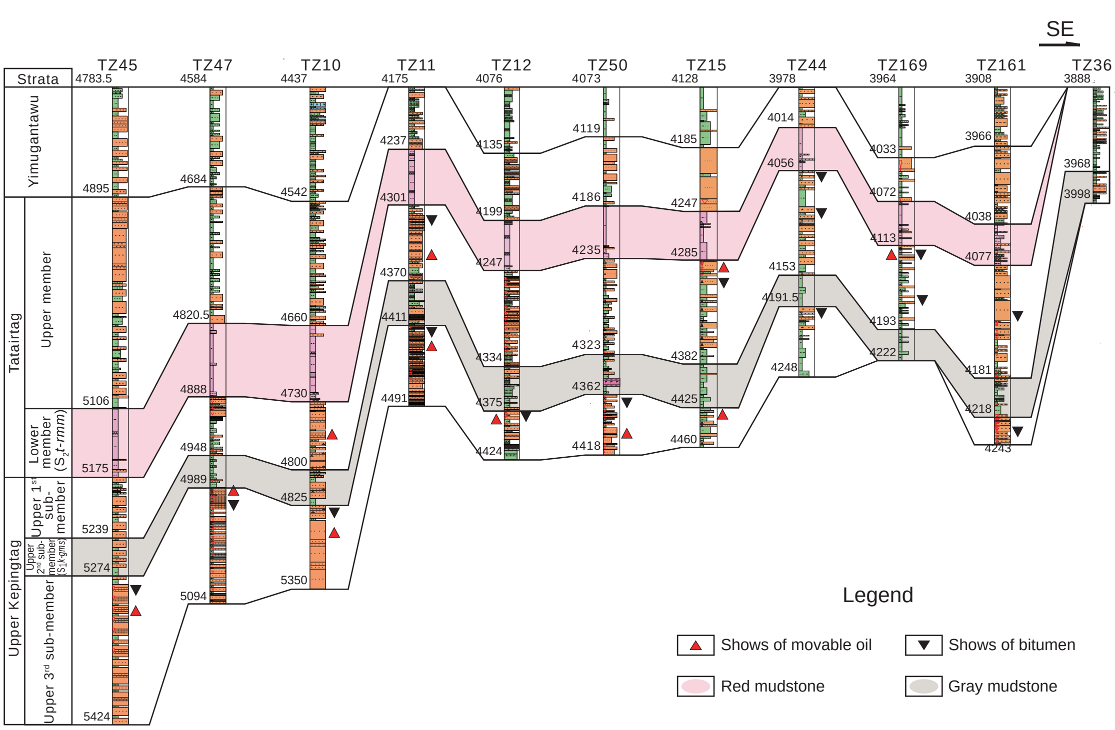


Fig. 8 Distribution profile of bituminous sandstone, movable oil and cap rock of the Silurian (see Fig. 3 for location)

Bitumen and heavy oil are widespread in $O_1y$ in the Central Fault Horst Belt, Tazhong Low Rise, where nearly 20 wells were drilled targeting carbonate buried hills of $O_1y$ and encountered widespread bitumen and heavy oil in weathering crust reservoir beds (Table 4). The area experienced Devonian uplifting, which led to erosion of the entire Middle and Upper Ordovician as well as part of Lower Ordovician. From then on, this area did not subside and receive sediment until the Carboniferous with the absence of marl cap rock in the 3rd to 5th members of $O_3l$ (Fig. 6). Hence large-scale uplifting resulted in destruction of $O_1y$ hydrocarbons charged in the earlier period (Lü et al, 2004; Zhang et al, 2011b).

Table 4 Oil and gas shows in the Central Faulted Horst Belt, Tazhong Low Rise

| Well | Top depth of weathering crust ($O_1$), m | Depth of coring interval, m | Core thickness, m | Fracture-cavity and oil and gas show |
|---|---|---|---|---|
| TZ2 | 3883.0 | 3872.2 - 3903.5 | 3.1 | Fissures developed and half-filled with asphalt. Small and medium holes developed with heavy crude outflow |
| TC1 | 4295.0 | 5065.8 - 5113.2 | 43.86 | Fissures developed, partly filled or half-filled with coaly asphalt. Holes developed with light crude outflow partly |
| TZ17 | 4116.0 | 4116.0 - 4143.6 | 27.6 | Fissures and holes developed, filled or half-filled with asphalt. Holes filled with asphalt |
| TZ61 | 3973.0 | 3975.0 - 3983.4 | 8.4 | Fissures developed, filled or half-filled with asphalt. Holes developed, partly filled with asphalt |

The discovered oil and gas in $O_1y$ is concentrated on the Tazhong Northern Slope. In addition to reservoir bed development and hydrocarbon migration, the $O_3l$ marl cap rock is also an important factor. According to updated exploration data, oil and gas of $O_1y$ are concentrated in the area with a marl thickness of more than 100 m, and the thicker the marl, the higher the gas/oil ratio (Fig. 6). Therefore, for the Tazhong Northern Slope with multiple phase hydrocarbon charging, earlier oil charging and later gas charging, the quality of cap rock is one of the factors determining gas/oil ratio in oil and gas bearing formations.

There is a difference in the development characteristics of the marl cap rock in $O_3l$ between the west and east of the Tazhong Northern Slope.

In the west of the Tazhong Northern Slope, there are no 4th and 5th members of $O_3l$, thus cap rock quality of marl in the 3rd member of $O_3l$ controls the vertical distribution of underlying hydrocarbons (Fig. 9). That is to say, to the west of ZG15 well, hydrocarbons could not accumulate in $O_1y$ below the 3rd member of $O_3l$ but migrated upward to the 2nd and 3rd members of $O_3l$, due to poor marl cap rock quality in the 3rd member of $O_3l$ with relatively low natural gamma, low shale content and low breakthrough pressure (there was a breakthrough in the sample of ZG19 well under the pressure of 7 MPa). While to the east of ZG15 well, hydrocarbons almost all accumulated in $O_1y$ below the 3rd member of $O_3l$, due to good cap rock quality of marl in the 3rd member of $O_3l$ with relatively higher natural gamma, higher shale content and higher breakthrough pressure (there was no breakthrough after 2 days in the sample of ZG8 well under the maximum pressure of 14 MPa).

In the east of the Tazhong Northern Slope, the marl cap rock in the 3rd to 5th members of $O_3l$ has a thickness of more than 200 m, meanwhile, there was no breakthrough after 2 days during breakthrough pressure testing of core samples from 8 wells under the maximum pressure of 14 MPa (Table 1). This indicates that marl cap rock in the 3rd to 5th members of $O_3l$ could seal the underlying hydrocarbons of $O_1y$ to form sizable $O_1y$ oil and gas accumulation.

## 4.4 Hydrocarbon accumulation versus $O_1y$ dense limestone cap rock

There is thick bedded dolomite with a thickness of around 700 m in $O_1p$ in the Tazhong Low Rise. Seismic profiles show obvious “string of beads” shaped seismic reflections along the top surface of $O_1p$ which represent the reflections of karst caves, vugs and fractures (Yuan et al, 2012). The overlying dense limestones without weathering in $O_1y$ act as cap rock for $O_1p$. The cap rock becomes thicker in the northeast part of the Tazhong Northern Slope near the Tazhong No.1 Fault, thus this area is favorable for exploration for $O_1p$ hydrocarbon.

Taking the TZ162 well as an example, with a top unconformity depth of $O_1y$ at 4,900 m, the depth of the karst reservoir bed controlled by the unconformity is 5,120 m from log interpretation; meanwhile, the depth of $O_1y$ bottom bed boundary with underlying $O_1p$ is 5,603 m, thus the dense limestone section from 5,120 m to 5,603 m in $O_1y$ with a thickness of 483 m could act as cap rock for underlying $O_1p$. In $O_1p$, acidizing testing for 5,931-6,050 m with a 9 mm nozzle produced 183,880 $m^3$ of gas. Therefore, the karst reservoir bed in $O_1p$ and the dense limestone section without weathering in $O_1y$ could form a good reservoir bed−cap combination.

## 4.5 Hydrocarbon accumulation versus Cambrian gypsum cap rock

There are high quality source rocks with a high abundance of organic matter in the Middle and Lower Cambrian around the Tazhong Low Rise. Meanwhile, the structures and dolomite reservoir beds below the Middle Cambrian gypsum cap rock are relatively well developed. Seismic data show

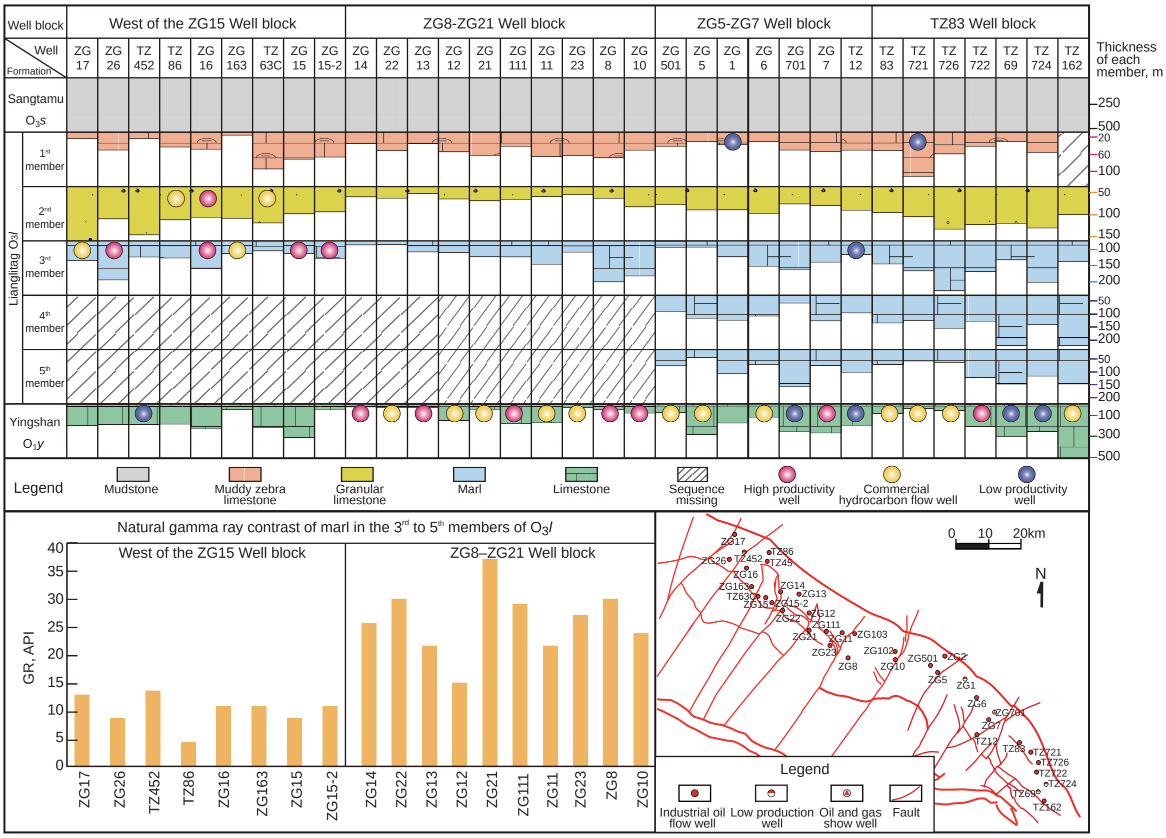


Fig. 9 Development characteristics of $O_3l$ cap rocks versus location of payzones on the Tazhong Northern Slope

that the Middle and Lower Cambrian salt-related structures are distributed in rows or belts along basement faults or fault-block belts in the Tazhong Low Rise (Tang et al, 2012).

The TC1 well penetrated the finely crystalline and silt-sized crystalline dolomites in the 7,085-7,162 m of Lower Cambrian. In parts of the core, vugs and fractures are well developed and are mostly half-filled or filled with crystal-clustered dolomite, bitumen or shale, while the largest vertical fracture is 0.33 m long and 2 mm wide and the largest vug is 35×12 mm. There was no oil smell when out of core barrel and some air bubbles emerged along the fractures.

In the Tazhong Low Rise, only the TC1 well in the east area penetrated through the Middle Cambrian gypsum, but the cap rock quality of gypsum in the central-west area should be better than the east area according to sedimentary characteristics. If this is confirmed by drilling, most probably sizable oil and gas could have been accumulated in the Lower Cambrian dolomites below the Middle Cambrian gypsum member.

## 5 Control on hydrocarbon accumulation by cap rocks

The Tarim Basin experienced complex tectonic movements and multi-phase hydrocarbon charging, and hydrocarbon accumulations were formed in multiple sets of reservoir bed–cap combinations. Research on the control of hydrocarbon accumulation by the Lower Palaeozoic cap rocks has to be combined with tectonic evolution, history of hydrocarbon generation and expulsion and hydrocarbon migration.

There are two sets of effective source rocks in the Cambrian-Lower Ordovician and the Middle-Upper Ordovician (Cai et al, 2009; Zhang et al, 2012). The Tazhong Low Rise experienced at least three periods of large-scale hydrocarbon accumulation: Late Caledonian–Early Hercynian, Late Hercynian and Himalayan (Zhang et al, 2011c; Pang et al, 2013).

The 1st period of large-scale hydrocarbon accumulation happened in the Late Caledonian − Early Hercynian, when the effective source rocks in Cambrian–Lower Ordovician of the Manjiaer Sag and Awati Sag adjacent to the north of the Tazhong Low Rise started large-scale hydrocarbon expulsion, and the Tazhong Low Rise was charged with hydrocarbon beginning from parts in the northwest and northeast (Zhang et al, 2011b). During the 1st period of hydrocarbon accumulation, $S_2t\text{-}rmm$ cap rock developed with its top surface at a maximum burial depth of 1,150-1,350 m (Fig. 10(a)) and highest palaeo-geotemperature of around 60 °C (Fig. 10(c), 10(d)), at sub-stage A of the early diagenetic stage.

The ages of the authigenic illite of the Silurian bituminous sandstones in the wells of TZ11 and TZ47 respectively are 364 Ma and 384 Ma, Early Hercynian (Zhang et al, 2011c). This suggests that the widespread Silurian bitumen in the Tazhong Low Rise evolved from the hydrocarbon accumulated during the 1st period of hydrocarbon accumulation. Meanwhile, almost all the Silurian bituminous sandstones were distributed below the $S_2t\text{-}rmm$ cap rock, suggesting that $S_2t\text{-}rmm$ cap rock with sealing capacity controlled vertical distribution of Silurian hydrocarbons (Zhang et al, 2004). In addition, the $O_3s$ mudstone cap rock also had sealing capacity at a top surface depth of 1,400-1,500 m (Fig. 10(b)).

Intense Devonian uplifting destroyed the hydrocarbons charged in the Late Caledonian–Early Hercynian. In the Central Fault Horst Belt and the east end area of the Tazhong Low Rise, the cap rocks including the mudstone of $S_2t$-*rmm*, the mudstone of $O_3s$ and the marl of $O_3l$ were completely denuded (Fig. 10(c), 10(d)). Meanwhile, in the remaining area of the Tazhong Low Rise, the cap rocks were preserved with $S_2t$-*rmm* mudstone at top surface depth of 200-800 m and $O_3s$ mudstone at top surface depth of 500-1,100 m (Fig. 10(a), 10(b)). When the burial depth of oil reservoirs was less than 1,500 m, crude oil was prone to suffering water washing oxidation and biodegradation (Larter et al, 2003). Meanwhile, the main strike-slip fault activity of the Tazhong area was sustained in the Early Hercynian (Li et al, 2013), thus tectonic uplifting and fault cutting resulted in the destruction of the Lower Paleozoic hydrocarbon reservoirs which were charged in earlier periods forming bitumen in sandstones and carbonates.

The 2nd period of large-scale hydrocarbon accumulation happened in the Late Hercynian. Permian volcanic activity resulted in a geothermal gradient of the Tarim Basin of up to 34-38 °C/km, thus the effective source rocks of Middle-Upper Ordovician in the west of the Manjiaer Sag started to expel oil at a large-scale then the hydrocarbon migrated into structural high areas along karstic carrier beds and unconformities from north to south and from northwest to southeast (Zhang et al, 2011b). During the 2nd period of hydrocarbon accumulation, $S_2t$-*rmm* and $O_3s$ mudstone developed with a top surface burial depth of 2,100-2,500 m and 2,350-2,800 m respectively (Fig. 10(a), 10(b)), all more than 2,000 m. Thereafter, there was no cap rock destruction by uplifting and denudation (Fig. 10(c), 10(d)), thus the accumulated hydrocarbons were well preserved. In addition, Ordovician reservoir beds in the Tazhong Low Rise experienced long-term and widespread karstification with well-developed dissolution pores, thus providing good space for large-scale oil expulsion and charging. This is why the discovered commercial oils in the Tazhong Low Rise were mainly generated from the Middle-Upper Ordovician source rocks (Zhang et al, 2000; Li et al, 2010; Zhang et al, 2011b; Tian et al, 2012).

The 3rd period of large-scale hydrocarbon accumulation

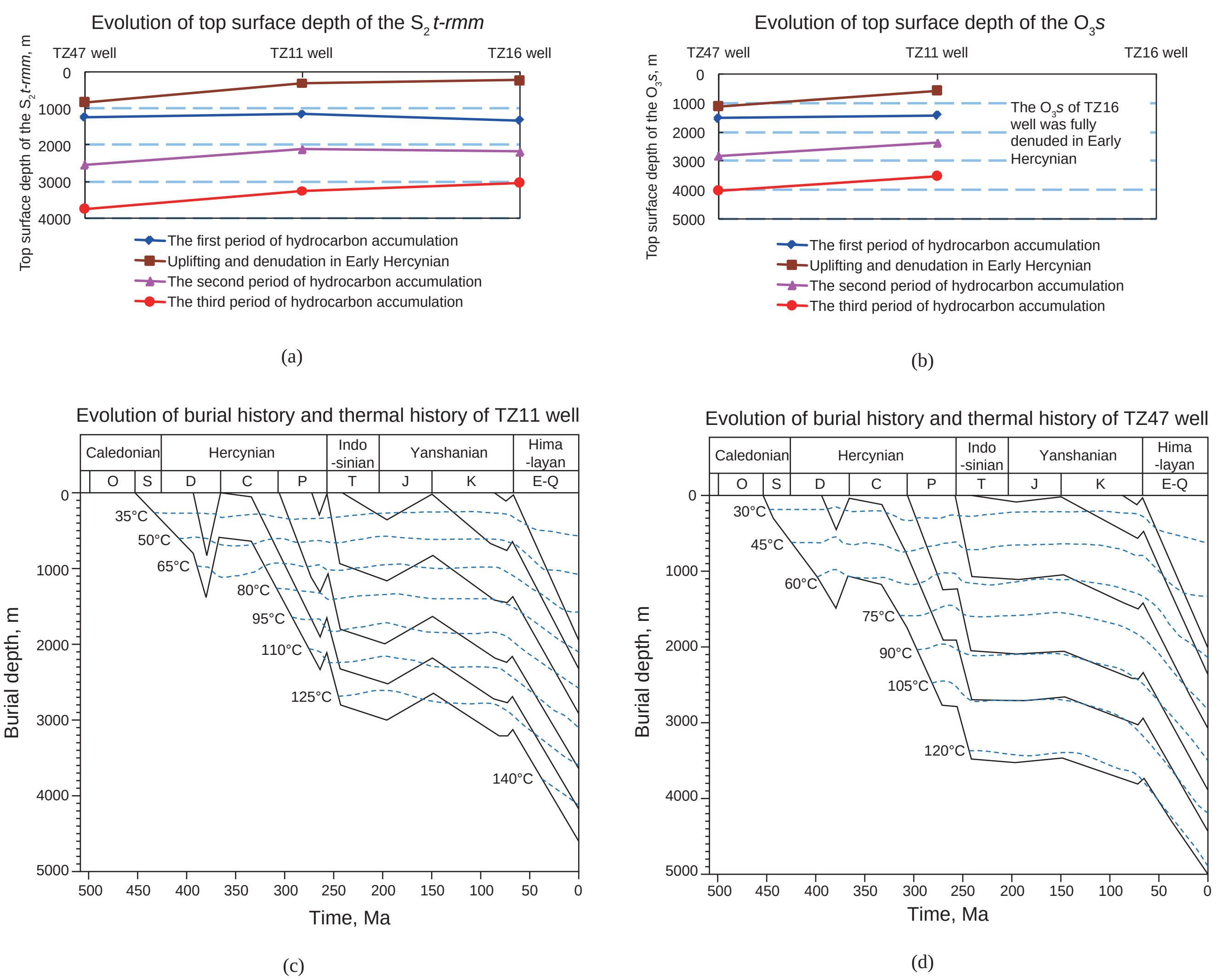


Fig. 10 Top depth change diagram of $S_2t$-*rmm* and $O_3s$ mudstone (attached with single well evolution diagrams of burial history and thermal history)

happened in the Himalayan. The Middle-Upper Ordovician effective source rocks in the slope area of the Tazhong Low Rise started to expel hydrocarbon, and the oil generated from the Cambrian-Lower Ordovician effective source rocks in earlier periods cracked into gas (Zhang et al, 2011b). Thus the accumulated Ordovician carbonate oil reservoirs were gradually altered by gas invasion from deep reservoirs, while the intersection of the Tazhong No.1 Fault with main strike slip faults acted as hydrocarbon charging points (Pang et al, 2013). On the Tazhong Northern Slope which was near the hydrocarbon charging points, the cap rocks of $O_3s$ mudstone and $O_3l$ marl were well preserved with relatively large thickness. In addition, during the 3rd period of hydrocarbon accumulation, $S_2t$-*rmm* and $O_3s$ mudstone developed with top surface burial depths of 3,000-3,750 m and 3,500-4,000 m respectively (Fig. 10(a), 10(b)), thus sizable condensate reservoirs were formed in the Ordovician carbonate along the Tazhong Northern Slope.

In structural high areas of the Central Fault Horst Belt and the east end of the Tazhong Low Rise, the Lower Paleozoic cap rocks were denuded by Devonian uplifting after the 1st period of large-scale hydrocarbon accumulation, resulting in the absence of regional sealing for hydrocarbons migrating in late periods. Therefore, there is no important discovery in the Lower Paleozoic after drilling 20 wells in the study area.

In summary, oil and gas accumulated in the Lower Palaeozoic during the early period of hydrocarbon accumulation were destroyed or degraded due to shallow burial depth of cap rocks; while oil and gas accumulated during late periods of hydrocarbon accumulation have been preserved due to suitable burial depth of cap rocks. The Tazhong Northern Slope with relatively well-preserved Lower Palaeozoic cap rocks and its location near hydrocarbon migration pathways is rich in oil and gas; while the Central Fault Horst Belt and the east end of the Tazhong Low Rise suffered denudation of Silurian and Ordovician cap rocks, and no important discovery has been made in the Lower Palaeozoic.

## 6 Conclusions

1) Several sets of effective local cap rocks are well preserved on the Tazhong Northern Slope despite the lack of regional cap rock covering the entire Tazhong Low Rise. The best cap rock is the mudstone of $O_3s$; the second is the mudstone of $S_2t$-*rmm* and the marl of $O_3l$; the third is the mudstone of $S_1k$-*gms*. The dense limestone of $O_1y$ and the gypsum of $\epsilon_2$ show sealing capacity, but their regional distributions are waiting for confirmation by drilling.

2) The Lower Palaeozoic effective cap rocks are closely related to hydrocarbon accumulation in the Tazhong Low Rise. The Tazhong Northern Slope near migration pathways and with well-preserved cap rocks is rich in Lower Palaeozoic hydrocarbons. However, the Central Fault Horst Belt and the east end of the Tazhong Low Rise suffered denudation of multiple sets of cap rocks, thus no large-scale discovery of hydrocarbons in the Lower Palaeozoic has been made there. Areally, Ordovician hydrocarbons are distributed in the areas where cap rocks including $O_3s$ mudstone and $O_3l$ marl are well-developed; vertically, most of reserves in the Tazhong Low Rise are distributed below $O_3s$ mudstone cap rock, and almost all bituminous sandstones and movable oils from the Silurian are concentrated below $S_2t$-*rmm* mudstone cap rock.

3) The Tazhong Low Rise experienced three periods of large-scale hydrocarbon accumulation and complex tectonic movements, and the evolution of Lower Paleozoic cap rocks controlled hydrocarbon accumulation. Taking cap rocks of $S_2t$-*rmm* and $O_3s$ mudstone as examples, in the Late Caledonian − Early Hercynian period of hydrocarbon charging, the cap rocks with top surface burial depths of 1,150-1,500 m could seal oil and gas; thereafter, with intense Devonian uplifting, the cap rocks with the top surface burial depths of 200-800 m and 500-1,100 m respectively were denuded in local areas, thus the hydrocarbons accumulated in earlier periods were degraded to widespread bitumen. In the Late Hercynian period of oil expulsion, the top surfaces of the cap rocks were at burial depths of 2,100-2,800 m and without denudation by uplifting thereafter, thus commercial oil accumulations were preserved. In the Himalayan period large-scale gas invasion occurred, and top surfaces of $O_3s$ mudstone were at burial depths of 3,500-4,000 m and without denudation by uplifting thereafter, thus sizable condensate reservoirs of $O_3l$ were formed.

4) The potential exploration targets in the Lower Paleozoic in the Tazhong Low Rise can be determined based on the characteristics of cap rocks. The first target is $O_1p$ below $O_1y$ dense limestone cap rock, because good dolomite reservoir beds developed in the top part of $O_1p$ or along the faults and accumulation of hydrocarbons have been confirmed by drilling. The second target is the Lower Dolomite Member below the $\epsilon_2$ gypsum cap rock, because the cap rock could be widespread in the entire Tazhong Low Rise, and salt-related structures and dolomite reservoir beds were relatively well developed. The regional distribution of gypsum cap rock is awaiting further confirmation. Combined with hydrocarbon migration, less risk would be involved in exploration on the Tazhong Northern Slope.

## Acknowledgements

This work was supported by the National Natural Science Foundation of China (No. 41072102), National Key Basic Research Development Plan (“973” Project, No. 2005CB422108) and National Major Projects (Nos. 2008ZX05004-004, 2011ZX05005-001).

## References

Cai C F, Li K K, Ma A L, et al. Distinguishing Cambrian from Upper Ordovician source rocks: Evidence from sulfur isotopes and biomarkers in the Tarim Basin. Organic Geochemistry. 2009. 40(7): 755-768

Chen R Y, Zhao W Z and Wang H J. Fluid inclusion evidence for charge stages of hydrocarbon in the Ordovician of Tazhong area, Tarim Basin. Petroleum Exploration and Development. 2010. 37(5): 537-542 (in Chinese)

Ding W L, Fan T L, Yu B S, et al. Ordovician carbonate reservoir fracture characteristics and fracture distribution forecasting in the Tazhong area of Tarim Basin, Northwest China. Journal of Petroleum

Science and Engineering. 2012. 86-87: 62-70
Escalona A and Mann P. An overview of the petroleum system of Maracaibo Basin. AAPG Bulletin. 2006. 90(4): 657-678
Gong S, George S C, Volk H, et al. Petroleum charge history in the Lunnan Low Uplift, Tarim Basin, China – Evidence from oil-bearing fluid inclusions. Organic Geochemistry. 2007. 38(8): 1341-1355
Hill K C. Structure of the Papuan Fold Belt, Papua New Guinea. AAPG Bulletin. 1991. 75(5): 857-872
Hill K C, Keetley J T, Kendrick R D, et al. Structure and hydrocarbon potential of the New Guinea Fold Belt. In: McClay K R (ed.), Thrust Tectonics and Hydrocarbon Systems: AAPG Memoir 82. Tulsa, Oklahoma: AAPG. 2004. 494-514
Ji Y G, Han J F, Zhang Z H, et al. Formation and distribution of deep high quality reservoirs of Ordovician Yingshan Formation in the Northern Slope of the Tazhong area in Tarim Basin. Acta Geologica Sinica. 2012. 86(7): 1163-1174 (in Chinese)
Jia C Z. Tectonic Characteristics and Petroleum, Tarim Basin, China. Beijing: Petroleum Industry Press. 1997. 279-283 (in Chinese)
Jia C Z and Li Q M. Petroleum geology of Kela-2, the most productive gas field in China. Marine and Petroleum Geology. 2008. 25(4-5): 335-343
Jiang Z X, Pang X Q, Liu L F, et al. Quantitative studies of hydrocarbon loss of the Silurian bitumen sandstone in the Tarim Basin. Science in China Series D: Earth Sciences. 2008. 51(S2): 101-107
Jin Z J and Wang Q C. Recent developments in study of the typical superimposed basins and petroleum accumulation in China: Exemplified by the Tarim Basin. Science in China Series D: Earth Sciences. 2004. 47(S2): 1-15
Larter S, Wilhelms A, Head I, et al. The controls on the composition of biodegraded oils in the deep subsurface—part 1: biodegradation rates in petroleum reservoirs. Organic Geochemistry. 2003. 34(4): 601-613
Li C X, Wang X F, Li B L, et al. Paleozoic fault systems of the Tazhong Uplift, Tarim Basin, China. Marine and Petroleum Geology. 2013. 39(1): 48-58
Li D S, Liang D G, Jia C Z, et al. Hydrocarbon accumulations in the Tarim Basin, China. AAPG Bulletin. 1996. 80(3): 1587-1603
Li S M, Li M W, Pang X Q, et al. Origin of crude oils with unusually high dibenzothiophene concentrations in the Tazhong Uplift, Tarim Basin. Journal of Geochemical Exploration. 2009. 101(1): 60
Li S M, Pang X Q, Jin Z J, et al. Petroleum source in the Tazhong Uplift, Tarim Basin: New insights from geochemical and fluid inclusion data. Organic Geochemistry. 2010. 41(6): 531-553
Lü X X, Fan Q H, Zhao F Y, et al. The Silurian play in the Tazhong Uplift, Tarim Basin, northwestern China. Marine and Petroleum Geology. 2007. 24(3): 189-198
Lü X X, Jin Z J, Liu L F, et al. Oil and gas accumulations in the Ordovician carbonates in the Tazhong Uplift of Tarim Basin, west China. Journal of Petroleum Science and Engineering. 2004. 41(1-3): 109-121
Lü X X, Zhang Y W and Jin Z J. Reservoir formation cycle of Tarim Basin, NW China. Chinese Science Bulletin. 1997. 42(3): 245-248
Meng Q Y, Pang X Q and Gao J B. The multi-factor recombination and processes superimposition model for hydrocarbon accumulation: application to the Silurian in the Tarim Basin. Petroleum Science. 2008. 5(1): 13-19
Pang H, Chen J Q, Pang X Q, et al. Key factors controlling hydrocarbon accumulations in Ordovician carbonate reservoirs in the Tazhong area, Tarim Basin, western China. Marine and Petroleum Geology. 2013. 43: 88-101
Pang X Q, Tian J, Pang H, et al. Main progress and problems in research on Ordovician hydrocarbon accumulation in the Tarim Basin. Petroleum Science. 2010. 7(2): 147-163
Qian Y X, He Z L, Chen Q L, et al. Sealing capacity of the Ordovician carbonate rocks in Tazhong area, the Tarim Basin. Oil & Gas Geology. 2012. 33(1): 1-9 (in Chinese)
Tang L J, Huang T Z, Qiu H J, et al. Salt-related structure and deformation mechanism of the Middle-Lower Cambrian in the middle-west parts of the Central Uplift and adjacent areas of the Tarim Basin. Science in China: Earth Sciences. 2012. 55(7): 1123-1133
Tian Y K, Zhao J, Yang C P, et al. Multiple-sourced features of marine oils in the Tarim Basin, NW China–Geochemical evidence from occluded hydrocarbons inside asphaltenes. Journal of Asian Earth Sciences. 2012. 54-55(2): 174-181
Wang F Y, Bian L Z, Zhang S C, et al. Two types of hydrocarbon generation organic matters in Ordovician marine source rocks, Tarim Basin. Science in China Series D: Earth Sciences. 2001. 31(2): 96-102 (in Chinese)
Wang X D, Jiang Z X, Pang X Q, et al. Comprehensive evaluation of sealing ability of Silurian cap rocks in Tarim Basin. Journal of Xi'an Shiyou University (Natural Science Edition). 2004. 19(4): 49-53 (in Chinese)
Yuan S Q, Jia C Z, Gao R S, et al. Sedimentation characteristics and reservoir geological model of Mid-Lower Ordovician carbonate rock in Tazhong northern slope. Acta Petrolei Sinica. 2012. 33(S1): 80-88 (in Chinese)
Zhang J, Pang X Q, Liu L F, et al. Distribution characteristics and petroleum geological significance of the Silurian asphaltic sandstones in Tarim Basin. Science in China Series D: Earth Sciences. 2004. 47(S2): 199-208
Zhang N, Tian L, Xing Y L, et al. Characteristics of hydrocarbon fluid inclusions and analysis of reservoir formation in Ordovician reservoirs of Tazhong area, Tarim Basin. Acta Petrologica Sinica. 2011a. 27(5): 1548-1556 (in Chinese)
Zhang S C, Gao Z Y, Li J J, et al. Identification and distribution of marine hydrocarbon source rocks in the Ordovician and Cambrian of the Tarim Basin. Petroleum Exploration and Development. 2012. 39(3): 305-314
Zhang S C, Hanson A D, Moldowan J M, et al. Paleozoic oil-source rock correlations in the Tarim Basin, NW China. Organic Geochemistry. 2000. 31(4): 273-286
Zhang S C, Zhang B M, Li B L, et al. History of hydrocarbon accumulations spanning important tectonic phases in marine sedimentary basins of China: Taking the Tarim Basin as an example. Petroleum Exploration and Development. 2011b. 38(1): 1-15
Zhang Y Y, Zwingmann H, Liu K Y, et al. Hydrocarbon charge history of the Silurian bituminous sandstone reservoirs in the Tazhong Uplift, Tarim Basin, China. AAPG Bulletin. 2011c. 95(3): 395-412
Zhu X M, Gu J Y, Jia J H, et al. Assessment of Reservoir and Cap Rock of the Key Strata Series in the Tarim Basin. Beijing: Petroleum Industry Press. 2003: 264-300 (in Chinese)

**(Edited by Hao Jie)**